Available online at www.sciencedirect.com
SCIENCE DIRECT
Bioorganic & Medicinal Chemistry 14 (2006) 3481–3490
Bioorganic & Medicinal Chemistry

Fluorescent intercalator displacement analyses of DNA binding by the peptide-derived natural products netropsin, actinomycin, and bleomycin

Mark A. Lewis and Eric C. Long*

Department of Chemistry and Chemical Biology, Purdue School of Science, Indiana University-Purdue University Indianapolis (IUPUI), 402 North Blackford Street, Indianapolis, IN 46202, USA

Received 26 October 2005; revised 4 January 2006; accepted 4 January 2006
Available online 24 January 2006

Abstract—The response of the high-throughput fluorescent intercalator displacement (HT-FID) assay reported recently by Boger et al. to peptide-based DNA binding intercalators and metal complexes was examined through the study of actinomycin and Co(III) · bleomycin-B_2. Along with a validation of netropsin that illustrated the good laboratory-to-laboratory reproducibility of the assay, our examination of actinomycin revealed results for a four base pair cassette library of DNA hairpins that paralleled the known DNA site-selectivity of this agent and also indicated the involvement of the flanking sequences of the hairpin oligonucleotide. In addition, for Co(III) · bleomycin-B_2 the established cleavage site-selectivity for 5′-GT and 5′-GC sites was correlated to drug-DNA association in this binding-only assay; our results also suggest a tetranucleotide site-selectivity for metallobleomycin involving cross-strand, 'back-to-back' 5′-GT and 5′-GC sites such as 5′-ACGT and 5′-ACGC.

1. Introduction

The high-throughput fluorescent intercalator displacement (HT-FID) assay developed recently by Boger et al. promises to complement existing, more technically demanding strategies to determine the DNA binding site-selectivities of low molecular weight molecules and other agents.[1,2] Indeed, the high-throughput nature of the FID assay is amenable to the screening of libraries of compounds and, unlike existing techniques[3] (e.g., footprinting and affinity cleavage) is capable of examining and rank-ordering the DNA binding site-selectivity of a single agent to all possible sequences simultaneously using a microplate format.[2] Conveniently, the FID assay also allows for a single DNA sequence of interest to be screened against a large number of compounds to discover low molecular weight ligands with particular binding properties.[4,5]

In brief, the FID assay[1,2] can assess the site-selectivity of a potential DNA binding ligand comprehensively by utilizing libraries of hairpin oligonucleotides containing a cassette of all possible 4- or 5-bp (or longer) sequences of interest; display of these libraries in a microplate format in the presence of the DNA intercalating fluorophores ethidium bromide or thiazole orange[6] results in sequence-dependent differential decreases in fluorescence upon introduction of a competing site-selective DNA binding agent to the wells of the microplate. The resulting changes in fluorescence caused by the presence of a particular DNA binding agent can then be rank-ordered for all the hairpin sequences and used as a HT means of determining relative site-selectivity. Conveniently, the rank-ordering determined by the HT aspect of the assay can be used to select DNA sequences (or DNA sequence-ligand pairs) of interest to examine in detail through quantitative FID titrations of individual hairpin oligonucleotides leading to a straightforward evaluation of binding affinity and stoichiometry.[1,2]

To date, the FID assay has been validated through the successful assessment of the DNA binding site-selectivities of several well-studied A/T-rich minor groove binding agents[2] including netropsin, distamycin, berenil, Hoechst 33258, and DAPI. In these cases, the assay revealed expected and new qualitative and quantitative insights into the preferences of these ligands for A/T-rich

Keywords: DNA; Fluorescence; Bleomycin; Actinomycin.
* Corresponding author. Tel.: +1 317 274 6888; fax: +1 317 274 4701; e-mail: long@chem.iupui.edu

0968-0896/$ - see front matter © 2006 Elsevier Ltd. All rights reserved.
doi:10.1016/j.bmc.2006.01.006

DNA regions, but now in a comprehensive fashion that cannot be provided easily by conventional footprinting. Along with the above, other linear, netropsin- and distamycin-like compounds have been assessed successfully by the FID assay including hairpin pyrrole–imidazole polyamides[7] and libraries of distamycin-like compounds.[4,5] Recent reports also have included examinations of the DNA binding affinity of triplex-forming oligonucleotides[8] and the assessment of the DNA binding affinity and selectivity of a protein, the lymphoid enhancer-binding factor (LEF-1).[9]

In our laboratory,[10,11] we have been examining the DNA recognition properties of libraries[12] of metallopeptides of the general form Cu(II)· or Ni(II) · Gly-Gly-His, where Gly can be any L- or D-α amino acid. During the course of these experiments we sought a further validation of the FID assay for low molecular weight peptide-derived agents and metal complexes that target ⩽4 bp DNA sites and G/C base pair-containing sites. Accordingly, we present the results of: (1) the validation of the FID assay in our hands using netropsin and, in doing so, illustrate the reproducibility of the assay and (2) an examination of two additional DNA binding peptide-derived antibiotics, actinomycin[13–15] and bleomycin[16] [Co(III) · bleomycin-B_2], using the HT-FID assay and subsequent quantitative titrations. While footprinting and other methods have been used to assess the site-selectivity of actinomycin, all possible sequences have not been examined, nor have the sequences examined via footprinting been compared equally within the same flanking sequence context. Additionally, with bleomycin, most information pertaining to the site-selectivity of this molecule has relied on an indirect assessment via the inherent DNA cleavage activity of this metallo-drug. Thus, the use of the HT-FID assay and a uniform hairpin sequence containing a cassette of four variable base pairs[6] provides a controlled environment of flanking sequences that may facilitate the comparison of the binding of each of these agents to all possible sequences. Of further interest, and perhaps as important, the compounds selected for study provide a basis for evaluating the response of the assay, and hairpin oligonucleotide library as designed initially, to well-established G/C-targeted small molecules and a validation of the FID technique for intercalating agents. Overall, it is hoped that the data presented will augment our current understanding of these peptide-derived agents and may be useful in expanding the utility of the FID assay to similar classes of yet unstudied compounds.

2. Results and discussion

2.1. Assay validation using netropsin

Initially, we sought to validate the FID assay in our own laboratory using netropsin, a well-studied A/T-rich minor groove binder, and available instrumentation that differed from that used in the development of the assay.[1,2] Given the well-behaved performance of netropsin in the assay, Boger et al. recommended its use in validation; netropsin was evaluated previously using the FID assay with both 4- and 5-bp cassette hairpin oligonucleotides and also through the use of ethidium bromide and thiazole orange as reporting fluorophores. Thus, adequate information exists for comparison. For our own validation of netropsin we carried out the assay using the four base pair cassette hairpins at a concentration of 1.5 μM hairpin-oligonucleotide and 4.5 μM ethidium bromide, as described previously.[6]

As shown in Figure 1, FID analyses of netropsin (at 0.75 and 1.5 μM) yielded merged-bar histograms of the rank-ordered 136 hairpin, four base pair library that, qualitatively, were virtually identical with regard to plot curvature in comparison to those produced earlier using ethidium bromide as the reporting fluorophore;[6] there is steep plot curvature associated with those hairpin sequences providing preferred binding sites for netropsin and the expected horizontal and vertical displacement of the FID profile as a function of increasing netropsin concentration. In our hands, the total percentage decrease in fluorescence observed for a given sequence was somewhat greater in comparison to that reported previously, but the variation observed was within the amount reasonably expected for an assay of this type.[17] Additionally, in developing the assay for our own studies we have chosen to color-code the results of the merged bar graph histogram: the ten A/T-*only*

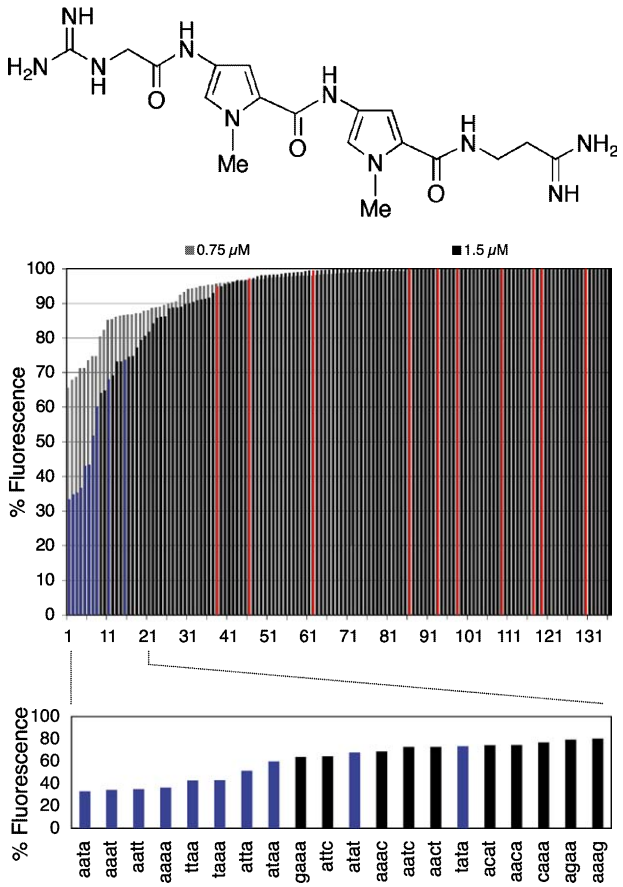

Figure 1. Structure of netropsin and merged-bar HT-FID histograms of netropsin at 0.75 and 1.5 μM drug concentrations.

four base pair sequences are color-coded blue and the ten G/C-*only* four base pair sequences are color-coded red while the mixed A/T and G/C-containing hairpin sequences remain black. We have found color-coding to be a very convenient means of visually assessing the gross differences between various DNA binding compounds and also establishing trends and patterns of selectivity. In the case of netropsin, a quick visual inspection of the FID plot clearly reveals the preferred A/T selectivity of this agent.

As noted above and illustrated further in Figure 1, for 1.5 μM netropsin, the A/T-only four base pair sequences (blue) provided preferred binding sites, as expected, with 9 (out of 10 possible) of these sequences found within the first 11 sequences selected in the rank-order. This result also is in accord with previous FID reports in which 9 of the top 10 hairpins selected consisted of A/T-only sequences when the same concentration of netropsin was employed in the assay. Examining more closely the actual sequences that constitute the top-ranked sites of netropsin binding, we find that the top four sequences observed in our analysis were also those selected in previous FID analyses of netropsin (5′-AATA, 5′-AAAT, 5′-AATT, and 5′-AAAA). Additionally, in both the present and previous FID studies, TATA was found to be the lowest-ranked of the A/T-only (blue) hairpin sequences and separated from the higher-ranked A/T-only sequences by several mixed A/T- and G/C-containing hairpin sequences. In further close correspondence with previous FID analyses, the mean rank ordering of the four base pair A/T sites was 6.2, while the mean position of the 3 bp A/T sites and 2 bp A/T sites were 29 and 82, respectively. Thus, as expected and noted previously, netropsin exhibited a 4 bp > 3 bp > 2 bp A/T selectivity.

While the HT-FID assay of netropsin revealed a rank-ordering of 136 bp hairpin sequences that closely reflected previous analyses, a true determination of rank-order requires quantitative titrations and Scatchard binding analyses to assess relative binding affinities, as noted.[2] As shown in Table 1 and the representative titration and Scatchard plot in Figure 2, quantitative FID analyses yielded relative binding affinities and stoichiometries that were in close correspondence to those reported earlier; in both the present and earlier FID studies of netropsin binding to the four base pair hairpin library, the top-ranked sequences were determined to be: 5′-AAAT > 5′-AAAA > 5′-AATT > 5′-AATA. Thus, while the absolute values of our experimentally determined binding affinities are somewhat lower than those

Table 1. Netropsin binding constants

FID rank	DNA sequence	K_a[a] ($\times 10^6$ M^{-1})	K_a[b] ($\times 10^6$ M^{-1})
2	5′-AAAT	88 (1.01)	127
4	5′-AAAA	58 (0.97)	92
3	5′-AATT	49 (1.03)	65
1	5′-AATA	42 (1.10)	64

[a] Scatchard analysis of titration binding curve (experimental stoichiometry of binding).
[b] Lit. FID analyses.[6]

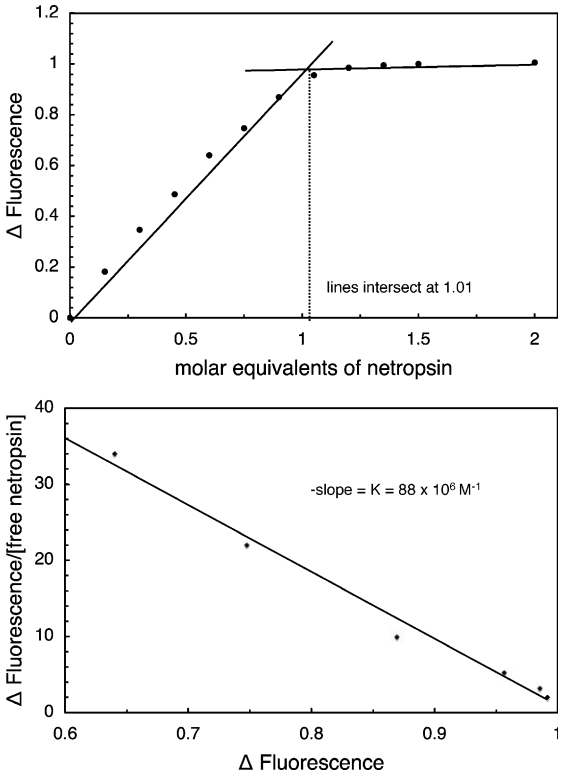

Figure 2. Representative quantitative titration and Scatchard binding analysis of netropsin in the presence of the 5′-AAAT four base pair cassette hairpin oligonucleotide.

reported earlier, perhaps more importantly they correspond identically with the rank-order established in previous FID studies. The above analyses validate the FID assay in our laboratory and also, notably, *attest to, and reveal, the high degree of laboratory-to-laboratory reproducibility that can be achieved by this assay*. These findings are important with regard to implementing the HT-FID assay in additional laboratories and extending its application to alternative classes of compounds, as constitutes the remainder of the work described herein.

2.2. Actinomycin

Actinomycin D is a clinically employed anticancer agent used in the treatment of various cancers.[18] While alternative DNA binding modes may contribute to the biological activity of this drug,[19–22] actinomycin D is believed to inhibit transcription by binding to double-strand DNA via intercalation of its phenoxazone ring into GpC.[13,23,24] The accepted basis for the GpC site-selectivity of actinomycin D derives from specific hydrogen bonding between the L-Thr carbonyl oxygens of the cyclic peptide drug moieties and both of the guanine 2-amino groups present in the minor groove of a duplex GpC dinucleotide step.[24–26] The resulting DNA–drug complex occupies a four base pair duplex sequence of the form 5′-X-GpC-Y and studies have indicated that the nucleotides present at X and Y can influence the affinity and dissociation kinetics of actinomycin D for these sites.[27–29] We show here that the HT-FID assay can be used conveniently to evaluate and rank order

actinomycin binding to all possible permutations of the 5′-X-GpC-Y site. In doing so, we also reveal aspects of the HT-FID assay that impact the study of G/C-targeted compounds.

Employing conditions as in our validation of netropsin, the merged-bar graph FID profiles for actinomycin (at 0.75, 1.5, and 3.0 μM drug concentrations) shown in Figure 3 exhibited plot curvature that was somewhat shallow and lacking the distinct shape indicative of netropsin-like site-selectivity. As emphasized through the 3.0 μM dataset, the FID profiles exhibit three 'tiers' of rank order consisting, approximately, of rank-ordered sequences: (1) 1–45; (2) 46–80; and (3) 81–136. Qualitative visual inspection indicates that this particular FID plot profile curvature is reminiscent of that reported for DAPI[2] and suggests that actinomycin is less selective toward the library, in total, in comparison to netropsin which targets the four base pair A/T-only sites almost exclusively out of a total of 136 hairpins. In further contrast to netropsin, the G/C-rich selectivity of actinomycin is immediately revealed in the color-coded FID profile: there is a distinct separation between the red bars of the G/C-only DNA hairpins and the blue bars of A/T-only DNA hairpins with the former contained approximately within the first two 'tiers' of the histogram and the latter, in stark contrast to netropsin, being contained within the lowest-ranked 'tier' of the histogram.

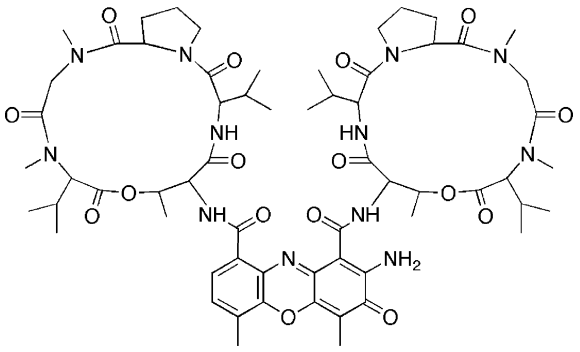

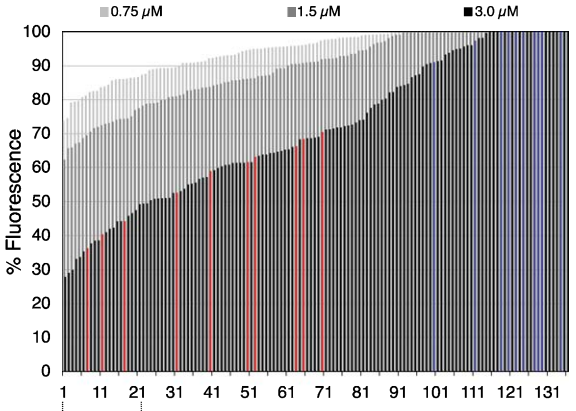

Rank	0.75 μM	1.5 μM	3.0 μM
1	CACG	CAGC	CACG
2	CAGC	CACG	CATG
3	CAGG	TGCA	CAGG
4	CATG	CATG	CAGC
5	TGCA	ACTG	TGCA
6	CGGC	CAGG	CAAG
7	CTAA	CGGC	CGCG
8	CAAC	CTAA	CCAG
9	CACA	CGGA	ACTG
10	ACTG	CACA	CGGC
11	CGCG	CTCA	CAAC
12	CACC	CGAA	CACC
13	CCCA	GGTA	CGAA
14	CGAA	CGCG	CTAA
15	CTAG	CACC	CTAG
16	GCAA	CAAC	CACA
17	AGCT	CCAG	CGCC
18	CCAG	CGCA	CGCA
19	CTCA	ATAG	CTCC
20	GGTA	CCCA	CGAG

Figure 3. Structure of actinomycin D and merged-bar HT-FID histograms of actinomycin at 0.75, 1.5, and 3.0 μM drug concentrations.

Focusing initially on the relative rank order of the four base pair cassettes containing *only* the 5′-X-GpC-Y sites documented as preferred by actinomycin (9 out of 10 of which appeared in the first tier of the rank-order), these hairpin sequences alone resulted in the histogram shown in Figure 4. In accord with previous studies of actinomycin,[20–31] our HT-FID results indicate that the 5′-X-GpC-Y sites ranked relative to one another in close agreement with binding assays and footprinting studies of this drug. Consistently, the preferred actinomycin binding site 5′-TGCA ranked in the FID top 5 for all assays that were carried out while 5′-GGCC, and other 5′-Pur-Pur-Pyr-Pyr sites, were lowest-ranked. Given the presence of all possible 5′-X-GpC-Y sites in the hairpin library, these data thus provide an independent, simultaneous verification of the relative influence of the nucleotides immediately flanking a GpC site on drug-DNA recognition,[25,27,28] but now in a directly comparable substrate context that is difficult to provide by other methodologies such as footprinting. Like others, we observe that 5′-Pyr-GpC-Pur (i.e., alternating Pyr-Pur-Pyr-Pur) is favored, while the presence of purine-purine steps appears less favored in the binding of actinomycin (as in 5′-Pur-GpC-Pyr or, more generally, 5′-Pur-Pur-Pyr-Pyr). The analysis described above also revealed a convenience of the HT-FID assay: the ability to selectively

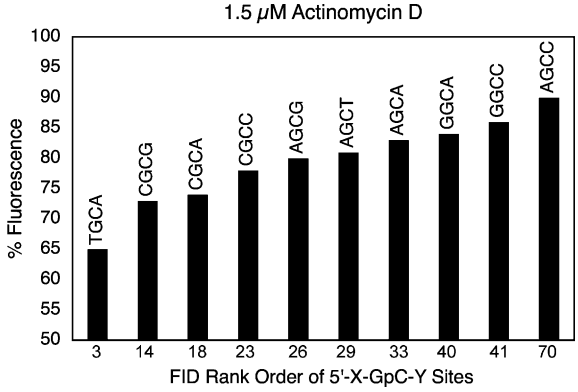

Figure 4. FID histogram of the rank-order of actinomycin (1.5 μM) binding to the four base pair 5′-X-GpC-Y cassette sites present in the oligonucleotide hairpin library.

examine and compare subsets of oligonucleotide sequences represented within the four base pair hairpin library.

As was discussed during the validation of netropsin, a true rank ordering of binding sites requires further quantitative comparison. To derive relative binding constants and verify the stoichiometry of drug binding to the typical 5′-X-GpC-Y four base pair cassettes shown in Figure 4, quantitative titrations and Scatchard analyses were carried out (Fig. 5). As reported in Table 2, quantitative FID titrations employing the ten 5′-X-GpC-Y four base pair cassette hairpins and subsequent Scatchard binding analyses established the rank-order of their actinomycin binding affinities and also their 1:1 binding stoichiometries. While some shuffling of the initial rank order determined by the HT-FID indeed occurred, the quantitative titrations, for the most part, confirmed the rank-order established by the plate assay; where changes in rank-order were observed, these changes occurred within hairpin sets that were initially rank-ordered closely within the shallow curvature of the profile.

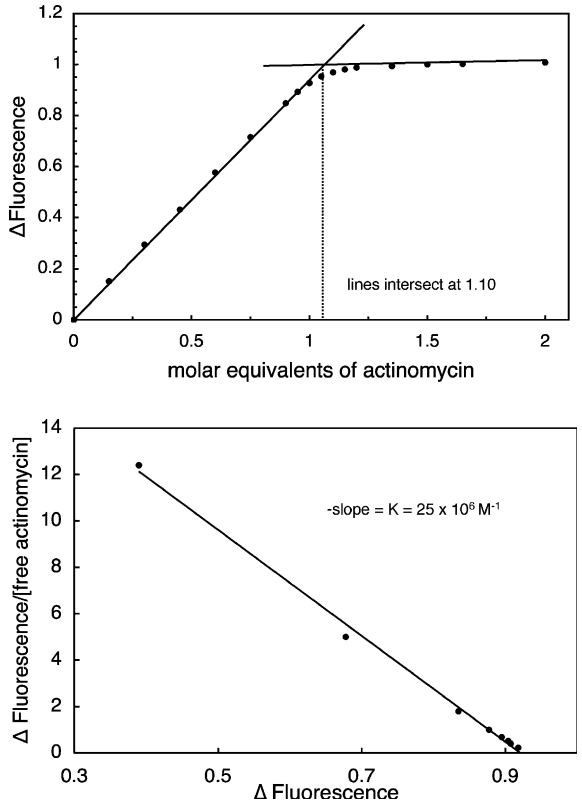

Figure 5. Representative quantitative FID titration and Scatchard binding analysis of actinomycin in the presence of the 5′-TGCA four base pair cassette hairpin oligonucleotide.

Table 2. Actinomycin binding constants

FID rank	DNA sequence	K_a[a] ($\times 10^6$ M^{-1})	K_a[b] ($\times 10^6$ M^{-1})
3	5′-TGCA	25 (1.12)	12.0
14	5′-CGCG	22 (1.11)	8.0
18	5′-CGCA	14 (1.11)	8.8
26	5′-AGCG	14 (1.05)	4.1
29	5′-AGCT	14 (1.03)	5.0
23	5′-CGCC	11 (0.98)	0.6
33	5′-AGCA	6 (0.92)	6.7
41	5′-GGCC	3 (0.96)	0.2
70	5′-AGCC	3 (1.02)	0.6
40	5′-GGCA	2 (0.94)	2.1

[a] Scatchard analysis of titration binding curve (experimental stoichiometry of binding).
[b] Lit. values (determined via absorbance titrations).[28,31]

Having established a close correspondence to previous studies of the site-selectivity of actinomycin among the 5′-X-GpC-Y four base pair cassette sites alone, why then was an apparent overall 'reduced' selectivity observed as indicated by the flattened FID profile in comparison to netropsin? This behavior can be explained by a close examination of the DNA hairpin library design (Fig. 6): actinomycin did not produce a sharp FID plot profile like that of netropsin because many of the DNA hairpins contained 5′-X-GpC-Y sites when the sequences of the flanks *overlapping* with the four base pair variable cassette are taken into consideration. These flanking 5′-X-GpC-Y steps lead to a redundancy of binding sites within the oligonucleotide hairpin library manifested as a 'flattening' of the overall FID curvature profile since many hairpins now afforded an equivalent response to drug binding. Indeed, 16 of the hairpin sequences that ranked in the top 20 contained a 5′-X-GpC-Y site in either flank of the four base pair variable cassette even when the four base pair cartridge of interest did not directly include one. In addition, the remaining hairpin oligonucleotide within the top 20 that did not contain a flanking nor a defined, four base pair 5′-X-GpC-Y cassette, 5′-GGTA (ranked 13th at 1.5 μM drug concentration), contained a GpG site also documented as supporting the binding of actinomycin.[29,30]

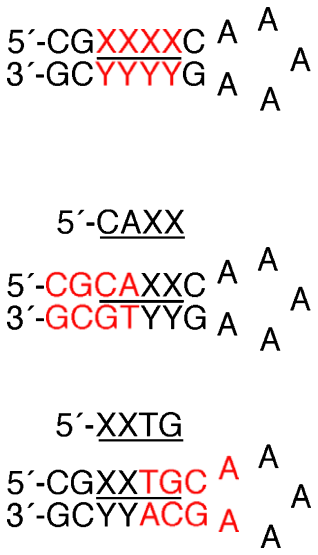

Figure 6. Actinomycin binding sites (red) within the hairpin oligonucleotide library used in this study; the four base pair cassette sites are underlined.

Upon further analysis, any hairpin that contained the four base pair cassette sequence 5′-CXXX (e.g., 5′-CAXX, see Fig. 6) also consequentially contained a 5′-X-GpC-Y site at the stem terminus because the complete hairpin stem sequence would then be 5′-CGCXXXC- (e.g., 5′-CGCAXXC-, as shown in Fig. 6). The presence of 5′-CAGC and 5′-CACG as the four base pair cassettes hairpins found in the first and second-ranked positions of the FID histogram of actinomycin (Fig. 3), respectively, supports the notion that the 5′-**CGCA** sites present at the stem termini of *both* of these library members are being targeted identically even though they do not contain comparable four base pair cassettes (i.e., within 5′-**CGCAGC**C- and 5′-**CGCACG**C; quantitative titrations also indicate equivalent binding, data not shown). As also illustrated in Figure 6, a similar circumstance may arise within hairpins containing the four base pair cassette sequence 5′-XXXG (e.g., 5′-XXTG as shown in Figure 6 and other four base pair cassette hairpins such as 5′-ACTG or 5′-ATAG) which generates the stem sequence: 5′-CGXXXGC*A*, where the 3′-terminal *A* is the first *unpaired* adenosine in the poly(A) loop of the hairpin construct. The duplex stem at its junction with the apical loop thus presents a 5′-X-GpC-*A* site to actinomycin. Interestingly, Hou et al. has documented that actinomycin D preferentially binds to GpC steps that are located adjacent to T:T mismatches.[20] While an A:A mismatch contained within a terminal loop, as in the present hairpin design, is indeed structurally different from a T:T mismatch contained within a duplex region of DNA, the consequential effect of widening of the DNA groove adjacent to the central GpC site, facilitating drug binding, likely exists in both cases. In addition, it is important to note that the hairpin oligonucleotides containing GpC steps outside of the four base pair variable cassette were likely rank ordered artificially high in the assay (relative to GpC sites contained fully within the duplex four base pair cassette 5′-X-GpC-Y sites) because of their proximity to the hairpin termini, which often favors drug-DNA binding and stacking.[19–22]

The above observations indicate that the hairpin oligonucleotides (without four base pair cassettes containing 5′-X-GpC-Y sites) that reported the binding of actinomycin can be accounted for in the FID profile in terms of known actinomycin binding sites through a careful consideration of the four base pair cassette in the context of the flanking sequence environment. The documentation of the response of this DNA binding agent to the original oligonucleotide library format,[1,6] as described herein, is important to the proper future use and application of the HT-FID assay. Thus, our results indicate the need for a careful interpretation of the data provided by the assay in light of: (1) the sequences *flanking* the four base pair variable cassette, especially when investigating an uncharacterized DNA binding agent and also (2) the *mechanism* of drug binding (i.e., groove binding vs intercalation). Additionally, in some instances it may be necessary to examine alternative hairpin sequences in those regions flanking the variable cassette of real interest to test their potential involvement. These results also point to the usual limitations inherent to the use of oligonucleotides as substrates that could present potential difficulties. Acknowledging and documenting the potential for such difficulties to arise is important for the proper application of this otherwise very powerful assay.

2.3. Bleomycin

The bleomycins constitute a group of glycopeptide-derived natural products isolated from *Streptomyces verticillus* that are clinically employed in the treatment of several cancers.[32] The generally accepted basis for the clinical efficacy of the bleomycins is believed to derive from their ability to mediate DNA strand scission in an Fe^{2+} and dioxygen dependent fashion, a process that produces both single- and double-strand DNA breaks with the latter thought to contribute significantly to the observed cytotoxicity of the drug.[16,32–34] The DNA cleavage activity of Fe(II) · bleomycin + O_2 is a selective process, DNA strand scission is initiated through the exclusive abstraction of C4′-H atoms mainly at pyrimidine nucleotides of sites containing 5′-GT and 5′-GC sequences.[16,32–34] Structurally, the DNA site-selectivity displayed by bleomycin is derived from the metal binding domain of the drug.[35,36] In particular, it has been shown that the pyrimidine moiety of Co(III) · bleomycin can form a nucleobase 'triplex' by association of its 4-amino and N3 nitrogens with the N3 and 2-amino groups of the guanine nucleobase within the minor groove of 5′-GC(T) sites.[32,36,37]

Much of what we know concerning the recognition of DNA by metallobleomycin has come via NMR studies of Co(III) · bleomycin 'green'.[16,37–39] This particular metallobleomycin contains a stable, metal-bound hydroperoxide moiety, and is thought to closely model the DNA binding behavior and ligand–metal interactions of the cleavage-active, and likely clinically relevant, Fe(II) · bleomycin + O_2 species. However, while detailed structural models of the interaction of metallobleomycin with selected DNA sites have been generated through the study of Co(III) · bleomycin,[36,37] most information regarding the binding site-selectivity of bleomycin, in general, has been gained through indirect studies of the DNA site-selective cleavage induced after the action of Fe(II) · bleomycin.[16,40,41] Thus, we have chosen the opportunity afforded by the HT-FID assay to examine metallobleomycin, Co(III) · bleomycin-B_2 in particular, in this binding-only assay. Co(III) · bleomycin derivatives are stable and do not mediate DNA strand scission in the absence of irradiation,[42] thus, in examining this metallobleomycin, binding events may be verified in the absence of cleavage chemistry. In doing so, these studies provide a validation of the FID assay for this form of metal-based DNA binding system, in general.

Employing HPLC-purified Co(III) · bleomyin-B_2 'green' at various concentrations in the HT-FID assay resulted in the merged-bar FID histograms shown in Figure 7. As illustrated, Co(III) · bleomycin exhibited FID plot curvature that was intermediate between that produced by netropsin and actinomycin; the sharp curvature found for metallobleomycin within the range of the

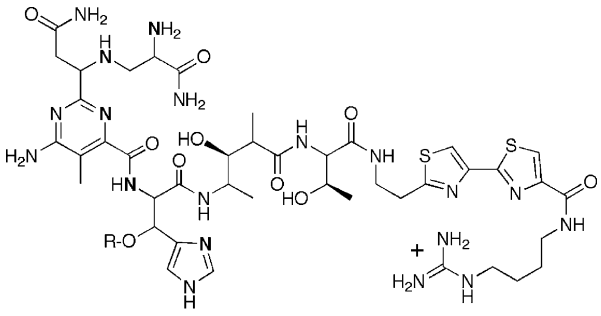

R = α-D-gulose-α-D-mannose disaccharide moiety; boldfaced nitrogens denote those involved in metal ion coordination

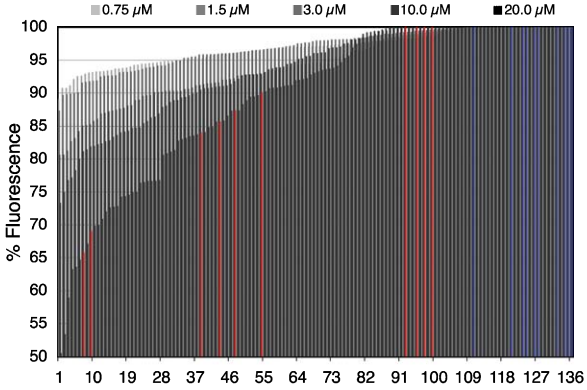

Rank	0.75 μM	1.5 μM	3.0 μM	10.0 μM	20.0 μM
1	**ACGT**	**ACGT**	**ACGT**	**ACGT**	**ACGT**
2	CACG	ACGC	ACGC	ACGC	AGTG
3	CGTC	CACA	AGTG	CACA	ACGC
4	ACAA	AGTG	CACG	AGTG	CACG
5	CGCG	CACG	CACA	CACG	CACA
6	ACCA	ACAC	AGCG	ACAC	ACAC
7	AGTA	AGCG	GTGA	AGCG	AGCG
8	GCAC	CGTC	CGCG	CGTC	CGCG
9	AGAG	AAGT	GGTA	AAGT	GAGC
10	ACCG	CGCG	ACAC	CGCG	GCGC
11	GTAA	GCAC	CGTC	GCAC	CGTC
12	AACG	GGTA	ACAA	GGTA	CACC
13	CACC	TACA	GACA	TACA	GACA
14	CACA	GTGA	AGAG	GTGA	AGAG
15	ATCG	AGTA	GAGC	AGTA	AACC
16	AGCG	CAGC	AGTA	CAGC	GTGA
17	GTAC	AGAG	AACG	AGAG	TACA
18	ATTC	GAGC	CACC	GAGC	ATGC
19	ACAT	ACAT	TACA	ACAT	AAGC
20	GAGC	AACG	CAGC	AACG	AGTA

Figure 7. Structure of apo-bleomycin-B_2 and merged-bar HT-FID histograms of Co(III) · bleomycin-B_2 at 0.75, 1.5, 3.0, 10, and 20 μM drug concentrations.

highest-ranked cassette sequences suggests that selectivity was achieved amongst the hairpins employed in the assay. Of immediate note, the separation observed between the red bars and blue bars indicates a preference for guanine sites over that of A/T-only sites/hairpins. In contrast, control FID experiments performed on apo-bleomycin and Co^{2+} salts alone (data not shown) failed to reveal an appreciable change in fluorescence or any discernable selectivity amongst members of the hairpin library.

Further analysis revealed that across the range of drug concentrations examined, within the top 15 ranked DNA hairpins, 14 contained at least two 5′-GT or 5′-GC dinucleotide sites (Fig. 7). Further scrutiny of the rank order revealed that the top 50% of the ranked hairpins all contain at least one 5′-GT or 5′-GC dinucleotide site in the duplex stem and, in contrast, only 16 out of the *lowest*-ranked 50% of the hairpins contained a 5′-GT or 5′-GC dinucleotide site. Thus, rank-order of a particular hairpin in the FID analysis of Co(III) · bleomycin correlates closely to the number of available 5′-GC/T dinucleotide sites. At this point it is important to note that the selectivity achieved in the HT-FID assay of Co(III) · bleomycin was found to be crucially dependent upon the buffer employed in the binding analysis: Tris · HCl buffers, as used in the HT-FID analyses of other DNA binding agents, failed to reveal a site-selective FID profile, while Na-cacodylate buffer consistently produced the profiles shown. The basis for this buffer dependence is unknown at present.

Perhaps of most interest is the observation that at 1:1 drug:hairpin concentrations and above (i.e., 1.5 to >20 μM bleomycin) the top five ranked hairpin cassette sequences found at the steepest portions of the FID profile where consistent and contained the sequences: 5′-ACGT, 5′-ACGC, 5′-CACA, 5′-AGTG, and 5′-CACG. Each of these sequences contains the well-established metallobleomycin cleavage sites 5′-GT and 5′-GC. In the case of the 5′-ACGT and 5′-ACGC cassettes, two of these preferred dinucleotide sites were contained within the same cassette. Particularly noteworthy, the results shown in Figure 7 also indicate that the drug preference for some of these sites was revealed at less than 1 equivalent of drug, suggesting a particularly strong selectivity for 5′-ACGT sites, which was revealed as being rank-ordered first at all concentrations studied. A cursory examination of the sequence of this particular four base pair cassette reveals it to contain two cross-strand, 'back-to-back' 5′-GT sites. Similarly, the four base pair cassette sequence 5′-ACGC, ranked second at most concentrations examined, also contains cross-strand, 'back-to-back' 5′-GT and 5′-GC sites.

The results described above suggest that while the HT-FID assay was able to easily reveal and confirm the dinucleotide preference of metallobleomycin, given that the top-ranked four base pair cassette sequences all contained at least one 5′-GT or 5′-GC preferred site of known bleomycin interaction, it was also able to reveal a particularly interesting *adjacent* site preference symmetry for this drug. Importantly, the 5′-ACGT site (and the similar 5′-ACGC site) suggests that drug binding may have some preference for tetranucleotide cassettes that enable the simultaneous adjacent, minor groove association of two bleomycin metal binding domains with the remainder of the drug displayed in opposite orientations relative to the minor groove. While speculation, such an interaction suggests that metallobleomycin binding may exhibit some level of cooperativity at particular DNA sites (i.e., binding of an initial metallobleomycin likely produces a minor groove structural environment conducive to a second, facilitated act of

drug binding). Aside from these two consistently top-ranked and unique sites, the remainder of the four base pair cassette hairpins found within the top 10–20 all contain single, isolated 5′-GT or 5′-GC sites, or adjacent, intrastrand dinucleotide sites that do not appear to elicit any particularly favorable drug response beyond that observed for isolated 5′-GT or 5′-GC sites.

Further quantitative analysis of metallobleomycin binding to the 5′-ACGT-containing hairpin confirmed its ability to bind two equivalents of drug. As shown in Figure 8, quantitative titration of Co(III) · bleomycin and the 5′-ACGT hairpin revealed a drug binding stoichiometry of ~2. In comparison, the four base pair cassette hairpin, 5′-GTAC, while of identical nucleotide composition to 5′-ACGT, but containing two dinucleotide sites in the opposite orientation, ranked considerably lower in this binding-only assay (36th at 1.5 μM and 42nd at 3 μM drug concentrations). Indeed, titration of this hairpin (Fig. 8) revealed a shallow plot without a clear binding stoichiometry and reflected the behavior of the other hairpin sequences ranked proximally. These results suggest that while the 5′-GTAC site is a documented 'hot spot' for double-strand DNA cleavage,[37] it does not appear to elicit any favored drug binding-only response beyond that observed for typical 5′-GT or 5′-GC sites. Thus, while the preferred 5′-ACGT and 5′-ACGC binding sites revealed in our investigation do not appear to impact the double-strand DNA cleavage model, they may nonetheless represent highly preferred sites of cooperative drug binding prior to cleavage as opposed to isolated or tandem dinucleotide sites.

Along with the above, the HT-FID profile revealed three conspicuous groupings of G/C-only red bars in the merged-bar histogram (Fig. 7) when a saturating amount of metallobleomycin (20 μM) was present. These groupings represent three different hairpin sequence 'classes'. The highest-ranked grouping contained the alternating purine–pyrimidine sequences 5′-GCGC and 5′-CGCG that constitute adjacent, preferred bleomycin binding sites; the second, middle-ranked grouping, contained hairpins with the cassettes 5′-CCGC, 5′-CGCC, 5′-CGGC, and 5′-GGCC with contiguous GpG sites and thus limited the number of available, bleomycin-preferred 5′-GC steps; and a third, lowest-ranked grouping, contained the sequences 5′-CCGG, 5′-CCCG, 5′-GCCC, and 5′-CCCC, predominated by homopolymeric G sequences that limited the number of dinucleotide steps preferred by bleomycin. Taking also into consideration the sequences of the G/C-nucleotides flanking these four base pair cassettes, the relative rank-ordering of the groupings described above is based simply on the number of available GpC steps contained in the entire hairpin: the highest-ranked group contained the greatest number of available bleomycin dinucleotide sites, while the lowest-ranked contained the least number of potential sites. This observation is consistent with the overall correlation between rank order of a hairpin and the number of available dinucleotide bleomycin binding sites noted earlier.

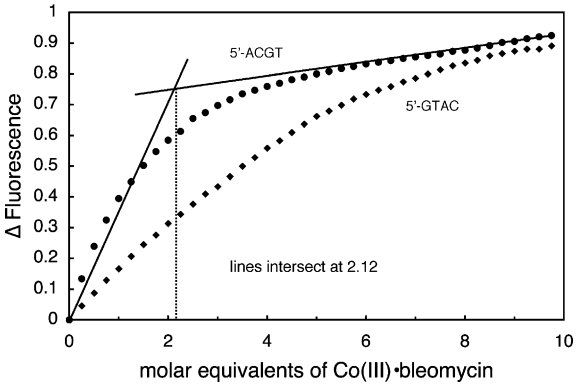

Figure 8. Quantitative FID titration of Co(III) · bleomycin-B_2 in the presence of the 5′-ACGT and 5′-GTAC hairpin oligonucleotides.

Overall, the above-described HT-FID analysis clearly correlates Co(III) · bleomycin-B_2 binding activity to the well-established site-selective DNA cleavage preferences exhibited by metallobleomycin. The sites revealed by the assay support also the validity of Co(III) · bleomycin as a good model for the activity of Fe(II) · bleomycin + O_2. Notably, the technique has also revealed an apparent binding preference for this drug to the 'back-to-back' tetranucleotide sites, 5′-ACGT and 5′-ACGC. For the purposes of assay development, this work also clearly validates the HT-FID assay for similar forms of DNA binding metal complexes.

3. Conclusions

The foregoing study has served to illustrate the exceptional laboratory-to-laboratory reproducibility that can be achieved with the HT-FID assay and has examined the response of the assay to two additional, as yet unstudied, DNA binding agents that have documented G/C site-selectivities. With netropsin, assay validation with this minor groove binder indicated that almost identical results could be achieved in comparison to the documented response of the HT-FID assay to this A/T-rich DNA targeted molecule. Our results support the use of netropsin as an important validating molecule for those wishing to establish the HT-FID assay in their own laboratories. In the case of actinomycin, the HT-FID assay exhibited a less selective response to this 5′-X-GpC-Y-targeted, intercalating molecule in comparison to netropsin. While the rank-order of the four base pair variable cassette DNA hairpins that contained 5′-X-GpC-Y sites reflected the predicted response to actinomycin binding, the flanking sequences of the hairpin oligonucleotides, as originally designed, were demonstrated to produce alternative sites that promoted the binding of actinomycin to other sequences contained within the 136-membered hairpin library; this response led essentially to 'false positive' results reflected in the shallow profile of the FID merged bar histogram. Importantly, our results document the response of the HT-FID assay, and the hairpin library as first designed, to this intercalating agent and indicate that the flanking sequences and mechanism of drug binding need to be considered in the interpretation of results from the

FID assay. Our results also point to the possibility of using alternative hairpin libraries with 'customized' flanking sequences once some level of information is achieved about an unknown DNA binding agent.

In examining the HT-FID response to Co(III) · bleomycin-B_2, we were able to demonstrate that DNA binding metal complexes of this type can be conveniently examined in the assay. The HT-FID assay verified that sites of binding correlate closely to sites of documented cleavage site-selectivity exhibited by Fe(II) · bleomycin + O_2 and also indicate that rank order of a particular four base pair cassette hairpin oligonucleotide correlates directly to the number of dinucleotide, 5′-GT, and 5′-GC sites contained within it. In addition to demonstrating that the HT-FID assay was able to reveal the site-selectivity of this dinucleotide-targeted agent, the four base pair variable cassettes employed in the assay revealed interesting tetranucleotide sites of metallobleomycin binding preference: 5′-ACGT and 5′-ACGC. These sites reflect the presence of two cross-strand, 'back-to-back' dinucleotide cleavage sites that appear to impart a preference for the binding of two equivalents of metallobleomycin; hairpin oligonucleotides with contiguous, intrastrand 5′-GT or 5′-GC sites, or even documented 'hotspots' for double-strand DNA cleavage by Fe(II) · bleomycin failed to elicit a similar, favorable binding response. Overall, these results, along with those obtained for actinomycin, indicate that the HT-FID assay is a valuable tool for discovery. Hopefully, documentation of the results described herein will enable others to similarly employ and advance the proper use of this assay.

4. Experimental

4.1. Materials

Netropsin and actinomycin were purchased from Sigma-Aldrich and quantitated spectroscopically.[43,44] Apo-bleomycin-B_2 was purchased from Calbiochem. Co(III) · bleomycin-B_2 was prepared from apo-bleomycin-B_2 and HPLC-purified as described previously;[39,45] ESI-MS confirmed and verified the purity of fractions containing Co(III) · bleomycin-B_2 green and brown which were quantitated spectroscopically as reported previously.[39,45] The 136-member hairpin deoxyoligonucleotide library was purchased from Trilink Biotechnologies, Inc. as individual lyophilized solids. Concentrations of the hairpin deoxyoligonucleotides were determined by the method described by Boger[2] using UV at 90 °C and single-strand extinction coefficients to ensure accurate concentration determination.

4.2. Fluorescent intercalator displacement assay

4.2.1. Netropsin and actinomycin. Each well of a Costar black 96-well plate was loaded with Tris buffer containing ethidium bromide (150 μL of 5.5 μM EtBr, 0.12 M NaCl, and 0.012 M Tris, pH 8.0 (identical results were obtained at pH 7.4)). To each well was added one hairpin deoxyoligonucleotide of the library (25 μL of 11.1 μM hairpin solution, 77.7 μM in base pairs, in H_2O). Final concentrations in each well were 1.5 μM DNA-hairpin, 4.5 μM EtBr, and 0.75 to 3 μM DNA binding agent. The final buffer consisted of 10 mM Tris, pH 8.0, 100 mM NaCl. After incubation at 25 °C for 30 min, each well was read (average of three readings) on a Varian Cary Eclipse fluorescence plate reader (λ_{Ex} 545 nm, λ_{Em} 595 nm). Compound assessments were conducted in triplicate (or more) with each well acting as its own control well (no agent = 100% fluorescence, no DNA = 0% fluorescence). Fluorescence readings are reported as a percent fluorescence decrease relative to the control wells.

4.2.2. Co(III) · bleomycin-B_2. The above protocol was followed exactly as stated, except for the substitution of Na-cacodylate buffer for Tris buffer using a range of drug concentrations (0.75–20 μM). The final analysis buffer consisted of 10 mM Na-cacodylate, pH 7.4 (or 8.0), 100 mM NaCl.

4.3. Quantitative FID titrations and determination of binding constants

A 400 μL quartz cuvette was loaded with Tris buffer (containing 100 mM NaCl and 10 mM Tris, pH 8.0) and ethidium bromide (4.5 μM final concentration). The fluorescence was measured on a Varian Cary Eclipse spectrofluorometer and normalized to 0% fluorescence. The hairpin deoxyoligonucleotide of interest was added (1.5 μM hairpin final concentration), and the resulting fluorescence was normalized to 100%. Titrations were conducted by adding aliquots of agent (1 μL, 0.15 μM in Tris buffer) and measuring the resulting fluorescence decrease after a 5 min equilibration time. Additions were continued until the system reached saturation and the fluorescence remained constant with subsequent additions of agent. In the case of Co(III) · bleomycin, the above protocol was used except that Na-cacodylate buffers were used exclusively (10 mM Na-cacodylate, pH 7.4, 100 mM NaCl). Using data provided by these titrations with select hairpin sequences, Scatchard binding analyses were performed for netropsin and actinomycin datasets exactly as described by Boger et al.[1,6]

Acknowledgment

We gratefully acknowledge the financial support of the National Institutes of Health (GM 62831 to E.C.L).

References and notes

1. Tse, W. C.; Boger, D. L. *Acc. Chem. Res.* **2004**, *37*, 61.
2. Boger, D. L.; Fink, B. E.; Brunette, S. R.; Tse, W. C.; Hedrick, M. P. *J. Am. Chem. Soc.* **2001**, *123*, 5878.
3. Fox, K. R. *Drug-DNA Interaction Protocols; Methods in Molecular Biology*; Humana: Totowa, NJ, USA, 1997; Vol. 90.
4. Boger, D. L.; Fink, B. E.; Hedrick, M. P. *J. Am. Chem. Soc.* **2000**, *122*, 6382.
5. Boger, D. L.; Dechantsreiter, M. A.; Ishii, T.; Fink, B. E.; Hedrick, M. P. *Bioorg. Med. Chem.* **2000**, *8*, 2049.

6. Boger, D. L.; Tse, W. C. *Bioorg. Med. Chem.* **2001**, *9*, 2511.
7. Tse, W. C.; Ishii, T.; Boger, D. L. *Bioorg. Med. Chem.* **2003**, *11*, 4479.
8. Yeung, B. K. S.; Tse, W. C.; Boger, D. L. *Bioorg. Med. Chem. Lett.* **2003**, *13*, 3801.
9. Ham, Y.-W.; Tse, W. C.; Boger, D. L. *Bioorg. Med. Chem. Lett.* **2003**, *13*, 3805.
10. Long, E. C.; Claussen, C. A. In *DNA and RNA Binders: From Small Molecules to Drugs*; Demeunyk, M., Bailly, C., Wilson, W. D., Eds.; Wiley-VCH: New York, 2003; pp 88–125.
11. Long, E. C. *Acc. Chem. Res.* **1999**, *32*, 827.
12. Huang, X.; Pieczko, M. E.; Long, E. C. *Biochemistry* **1999**, *38*, 2160.
13. Waring, M. J. *Annu. Rev. Biochem.* **1981**, *50*, 159.
14. Gale, E. F.; Cundliffe, E.; Reynolds, P. E.; Richmond, M. H.; Waring, M. J. In *The Molecular Basis of Antibiotic Action*, 2nd ed.; Wiley: London, 1981; pp 258–401.
15. Waring, M. J. In *Molecular Aspects of Anticancer Drug-DNA Interactions Vol. 1*; Neidle, S., Waring, M. J., Eds.; Macmillan: London, 1993; pp 213–242.
16. Claussen, C. A.; Long, E. C. *Chem. Rev.* **1999**, *99*, 2797.
17. Some potential technical differences that may slightly alter the response of the FID assay as carried out in our laboratory versus that of Boger included larger sample volumes in the 96-well plate, instrument configuration and plate alignment, and slight λ_{max} differences in EthBr due to experimental variability in solution conditions.
18. Yang, X.-L.; Wang, A. H.-J. *Pharmacol. Ther.* **1999**, *83*, 181–215.
19. Chen, F.-M.; Sha, F.; Ko-Hsin, C.; Shan-Ho, C. *Nucleic Acids Res.* **2004**, *32*, 271.
20. Hou, M.-H.; Robinson, H.; Gao, Y.-G.; Wang, A. H.-J. *Nucleic Acids Res.* **2002**, *30*, 4910.
21. Snyder, J. G.; Hartman, N. G.; D'Estantoit, B. L.; Kennard, O.; Remeta, D. P.; Breslauer, K. P. *Proc. Natl. Acac. Sci. U.S.A.* **1989**, *86*, 3968.
22. Sha, F.; Chen, F.-M. *Biophys. J.* **2000**, *79*, 2095.
23. Muller, W.; Crothers, D. M. *J. Mol. Biol.* **1968**, *35*, 251.
24. Kamitori, S.; Takusagawa, F. *J. Mol. Biol.* **1992**, *225*, 445.
25. Jennewein, S.; Waring, M. J. *Nucleic Acids Res.* **1997**, *25*, 1502.
26. Sobell, H. M.; Jain, S. C. *J. Mol. Biol.* **1972**, *68*, 21.
27. Chen, F.-M. *Biochemistry* **1988**, *27*, 1843.
28. Chen, F.-M. *Biochemistry* **1988**, *27*, 6393.
29. Goodisman, J.; Rehfuss, R.; Ward, B.; Dabrowiak, J. C. *Biochemistry* **1992**, *31*, 1046.
30. Van Dyke, M. W.; Herzberg, R. P.; Dervan, P. B. *Proc. Natl. Acad. Sci. U.S.A.* **1982**, *79*, 5470.
31. Chen, F.-M. *Biochemistry* **1992**, *31*, 6223–6228.
32. Chen, J.; Stubbe, J. *Nat. Rev. Cancer* **2005**, *5*, 102.
33. Hecht, S. M. *J. Nat. Prod.* **2000**, *63*, 158–168.
34. Boger, D. L.; Cai, H. *Angew. Chem. Int. Ed.* **1999**, *38*, 449.
35. Carter, B. J.; Murty, V. S.; Reddy, K. S.; Wang, S.-N.; Hecht, S.-M. *J. Biol. Chem.* **1990**, *265*, 4193.
36. Stubbe, J.; Kozarich, J. W.; Wu, W.; Vanderwall, D. E. *Acc. Chem. Res.* **1996**, *29*, 322.
37. Vanderwall, D. E.; Lui, S. M.; Wu, W.; Turner, C. J.; Kozarich, J. W.; Stubbe, J. *Chem. Biol.* **1997**, *4*, 373.
38. Xu, R. X.; Nettesheim, D.; Otvos, J. D.; Petering, D. H. *Biochemistry* **1994**, *33*, 907.
39. Wu, W.; Vanderwall, D. E.; Lui, S. M.; Tang, X.-J.; Turner, C. J.; Kozarich, J. W.; Stubbe, J. *J. Am. Chem. Soc.* **1996**, *118*, 1268.
40. D'Andrea, A. D.; Haseltine, W. A. *Proc. Natl. Acad. Sci. U.S.A.* **1978**, *75*, 3608.
41. Takeshita, M.; Grollman, A. P.; Ohtsubo, E.; Ohtsubo, H. *Proc. Natl. Acad. Sci. U.S.A.* **1978**, *75*, 5983.
42. Saito, I.; Morii, T.; Sugiyama, H.; Matsuura, T.; Meares, C. F.; Hecht, S. M. *J. Am. Chem. Soc.* **1989**, *111*, 2307.
43. Lah, J.; Vesnaver, G. *Biochemistry* **2000**, *39*, 9317.
44. Bailly, C.; Kenani, A.; Waring, M. *J. Nucleic Acids. Res.* **1997**, *25*, 1516.
45. Rajani, C.; Kincaid, J. R.; Petering, D. H. *J. Am. Chem. Soc.* **2004**, *126*, 3829.